



In-silico Design of Multi-epitope Vaccine for Tackling Type-1 Parainfluenza Virus

Zaid Khan^{1*}, Sana Sumera², Mekkanti Manasa Rekha³

Abstract

Human parainfluenza viruses (HPIV) often cause breathing infections, particularly in kids and infants. HPIV-1 is known for causing severe croup, yet no approved vaccines exist for HPIV infections. This study employed an *in-silico* approach to design a potential vaccine candidate targeting the fusion glycoprotein antigen of HPIV-1. Results highlighted that B-cell and T-cell epitopes were successfully identified from the fusion glycoprotein antigen using *in-silico* methods. Epitopes passing antigenicity, allergenicity, and toxicity assessments were selected and connected using appropriate linkers. The constructed vaccine exhibited favorable physiochemical properties, structural stability, and strong binding affinity with the TLR (Toll like receptor)-8. The vaccine sequence was successfully cloned into the pET-28a (+) vector. In Conclusion This study presents a promising development in the quest for an effective HPIV-1 vaccine. The design and construction of the multi-epitope vaccine, along with its structural validation, provide a solid foundation for further research. However, additional *in vitro* and *in vivo* investigations are crucial to assess the vaccine's efficacy, immunogenicity, and safety prior to clinical application.

Keywords: Human parainfluenza virus, Antigen, *In-silico* vaccine design, *In-silico* cloning

INTRODUCTION

Background

Human parainfluenza viruses (HPIVs) are enveloped, negative-stranded RNA viruses belong to paramyxoviridae family. These viruses comprise four serotypes, including HPIV-1, HPIV-2, HPIV-3, and HPIV-4, and are known to cause infections in both the upper and lower respiratory tracts. HPIVs are a significant cause of respiratory illnesses worldwide, particularly among infants, young children, and immunocompromised individuals [1]. The HPIV genome consists of a single negative RNA strand

that encodes six essential proteins, namely the matrix protein (M), the phosphoprotein (P), the fusion glycoprotein (F), the hemagglutinin-neuraminidase (HN) glycoprotein, the RNA polymerase (L), and the nucleocapsid protein (NP). These proteins play crucial roles in viral replication, assembly, and host immune response modulation [2]. The first identification of human parainfluenza virus dates back to 1955 when it was isolated from children with croup, a respiratory condition characterized by coughing, hoarseness, and difficulty breathing. Following that, HPIV became recognized as a huge contributor to respiratory tract infections in children. The severity and effects of HPIV infections can range based on the virus's serotype and the precise geographic place. For instance, HPIV-1 is well-known for causing pediatric laryngotracheobronchitis (croup) and is

*Author for Correspondence

Zaid Khan

E-mail: zaidkhan9515@gmail.com

¹Researcher, Department of Pharmacy Practice, Aditya Bangalore Institute of Pharmacy Education and Research, Bangalore, India

²Researcher, Department of Pharmacy Practice, Aditya Bangalore Institute of Pharmacy Education and Research Bangalore, Karnataka, India

³Associate Professor, Department of Pharmacy practice, Aditya Bangalore Institute of Pharmacy Education and Research, Bangalore, Karnataka, India

Received Date: October 16, 2023

Accepted Date: October 20, 2023

Published Date: November 03, 2023

Citation: Zaid Khan, Sana Sumera, Mekkanti Manasa Rekha. *In-silico* Design of Multi-epitope Vaccine for Tackling Type-1 Parainfluenza Virus. Research & Reviews: A Journal of Bioinformatics. 2023; 10(2): 30–46p.

responsible for nearly 30,000 hospitalizations annually in the United States alone [3]. Infections caused by HPIV-2 and HPIV-3 are associated with a range of respiratory illnesses, including bronchitis, bronchiolitis, pneumonia, and upper respiratory tract infections. Infants and young children are particularly susceptible to acute respiratory diseases caused by HPIVs. Primary infections often involve the lower respiratory tract and can manifest as severe illnesses, especially in individuals with underlying medical conditions or compromised immune systems. By the age of five, approximately 80% of children test positive for HPIV-1, HPIV-2, or HPIV-3. While most cases of HPIV infection can be managed in an outpatient setting, severe infections may require hospitalization [4, 5]. The pathogenesis of HPIV infections typically begins with the exposure of respiratory epithelial cells to the virus through contact or inhalation. HPIV primarily replicates in respiratory epithelial cells and does not spread systemically. The viruses enter host cells by binding to specific receptors on the cell surface, followed by fusion of the viral envelope with the host cell membrane. This fusion process is facilitated by the viral F protein, which undergoes conformational changes to mediate fusion of the viral envelope with the target cell membrane. The HN glycoprotein, on the other hand, plays a crucial role in viral attachment and release by binding to sialic acid-containing receptors on the host cell surface. The clinical manifestations of HPIV infection can vary depending on the serotype, viral load, and host immune response. Common symptoms include fever, cough, rhinorrhea, sore throat, and difficulty breathing. In more severe cases, lower respiratory tract involvement can lead to bronchiolitis, pneumonia, and respiratory distress, particularly in young infants. In immunocompromised individuals, HPIV infections can cause significant morbidity and mortality. The immune response to HPIV consists of both innate and adaptive components. Innate immune cells recognize viral components through pattern recognition receptors, leading to the production of pro-inflammatory cytokines and the recruitment of immune effector cells. This early immune response is critical for limiting viral replication and initiating the adaptive immune response. Adaptive immunity, including both humoral and cellular responses, plays a central role in clearing the infection and providing long-term protection against reinfection. Antibodies targeting the F and HN glycoproteins are crucial for neutralizing viral particles and preventing viral attachment and entry into host cells. Cellular immune responses, particularly CD8+ and CD4+ T cells, contribute to viral clearance and the resolution of infection [6, 7]. Despite the substantial burden imposed by HPIV infections, there is currently no available vaccine. Therefore, the development of an effective preventive strategy is of utmost importance. Traditional vaccine development approaches using live-attenuated or inactivated whole-virus vaccines have faced challenges due to safety concerns and the difficulty in achieving optimal immunogenicity. To overcome these limitations, alternative vaccine strategies such as subunit vaccines, viral-vectored vaccines, and nucleic acid-based vaccines have gained attention [8]. In recent years, in-silico approaches and computational tools have emerged as valuable tools in vaccine design and development. These methods allow for the identification and selection of specific viral epitopes that can elicit a robust immune response. By utilizing bioinformatics tools, researchers can predict potential B-cell and T-cell epitopes within viral proteins, analyze their immunogenicity, and evaluate their potential as vaccine candidates. This in-silico approach offers advantages such as reduced experimental cost and time, rational design based on immunoinformatics principles, and the ability to tailor vaccines for specific populations or viral variants [9]. In this study, we employed a computational approach to design an in-silico multi-epitope vaccine candidate against the human parainfluenza virus. Specifically, we focused on the F glycoprotein as antigenic target for vaccine design. The F protein is a critical determinant of viral entry into host cells. By targeting this glycoprotein, we aimed to create a vaccine that could confer long-term immunity against HPIV infections and potentially mitigate the associated morbidity and mortality. The present study presents a comprehensive workflow, as depicted in Figure 1, outlining our computational approach to vaccine design. Through the use of bioinformatics tools and immunoinformatics algorithms, we identified potential B-cell and T-cell epitopes within the F glycoprotein. These epitopes were carefully selected based on their predicted antigenicity, allergenicity and toxicity evaluation. Furthermore, we incorporated appropriate adjuvants and linkers to optimize vaccine efficacy and stability. Finally, the constructed vaccine was docked with TLR 8, and simulation was used to estimate its effectiveness and stability.

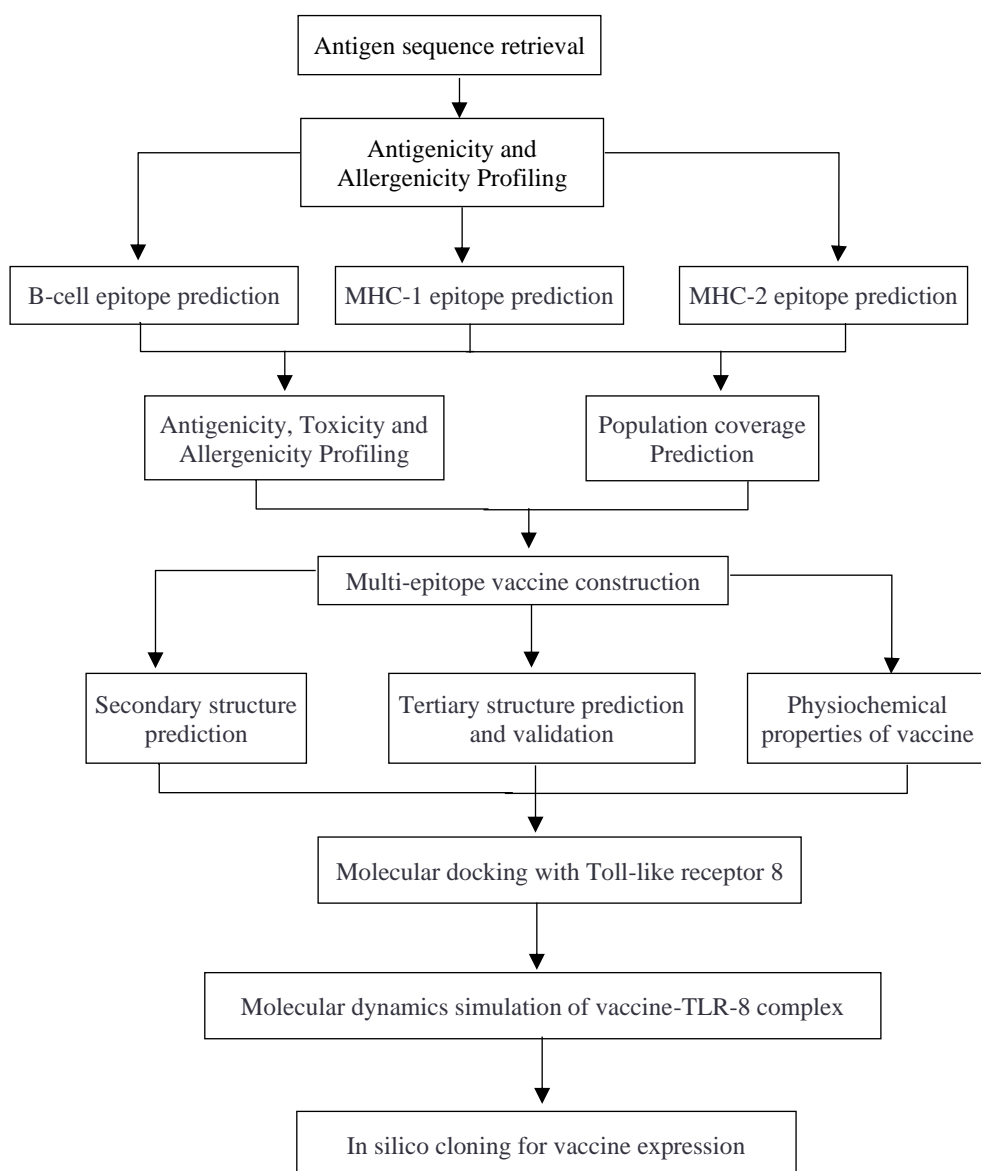


Figure 1. Workflow of the current study.

MATERIALS AND METHODS

Selection of Antigen and its Sequence Retrieval

The F(Fusion) glycoprotein of the human parainfluenza virus plays a critical role in virus-host cell membrane fusion. This glycoprotein helps the virus to permit the viral nucleocapsid to enter a host cell. Also, this protein is required for membrane fusion between cells and causes haemolysis [10]. Antibodies to fusion glycoprotein play a vital role in the establishment of immunity. Hence, we selected HPIV (strain C39) and its fusion glycoprotein F0, the sequence of Fusion glycoprotein was retrieved from the Uniprot web server (<https://www.uniprot.org/>) having Uniprot ID P12605 [11].

Antigenicity Prediction of Protein Sequence

It is an important aspect of vaccine development that the vaccine candidate should have more antigenic properties. The VaxiJen server includes the antigenicity of bacterial, viral, and tumor models. In this server, the protein sequence of Fusion glycoprotein was submitted in fasta file format (<https://www.ddg-pharmfac.net/vaxijen/VaxiJen/VaxiJen.html>). The results page displays the selected target, the protein sequence, the probability of its prediction, and a statement of whether it is a protective antigen or non-antigen based on a predefined cutoff of 0.5 [12].

Allergenicity and Toxicity Prediction of Protein Sequence

The recognition of allergens is also an essential step in the development of vaccines. The AllerTop v.2.0 server was used to predict the allergenic characteristics (<https://www.ddg-pharmfac.net/AllerTOP/>). In this server, the protein sequences were submitted in fasta format. The allergen status is returned on the results page as "Probable Allergen" or "Probable Non-allergen". On this basis, AllerTOP v.2.0 determines the most likely route of exposure for tested proteins predicted to be allergens [13]. We predicted the toxicity with the aid of the ToxinPred server, which determines whether the protein sequence is toxic or not (<https://webs.iitd.edu.in/raghava/toxinpred/protein.php>) [14].

B Cell Epitopes Prediction

B cell epitopes are fundamental for stimulating a humoral immune reaction, they activate the B-lymphocytes for the generation of antibodies and because of this factor, it plays an important part in vaccine design. We used the IEDB B-cell epitope prediction server (<http://tools.iedb.org/bcell/>) for the identification of linear B-cell epitopes, in that server we chose Bepipred Linear Epitope Prediction 2.0 method. Further, the epitopes were tested for antigenicity, allergenicity, and toxicity profiling, which were utilized for the construction of the vaccine [15].

T-cell Epitopes Prediction

The MHC (Major Histocompatibility Complex)-1 and MHC-2 epitopes were predicted by the IEDB server (<https://www.iedb.org/>) [16]. These epitopes are important because the vaccine should have the capacity to bind the MHC protein. On this server homepage, there is a specific tool for predicting MHC-1 and MHC-2 epitopes. For the prediction of MHC-1 epitopes, we used the IEDB MHC-1 server (<http://tools.iedb.org/mhci/>). Here, we used the ANN 4.0 prediction method and set the source species as human and selected the HLA allele reference set. MHC-2 epitopes were predicted using the IEDB MHC-2 server (<http://tools.iedb.org/mhcii/>). For this, NN-align 2.3 (Net MHC II 2.3) was used, the species was selected as human, the full HLA reference set and its length was selected as default. The MHC-1 and MHC-2 epitopes were tested for antigenicity, allergenicity, and toxicity profiling. Population coverage of both MHC-1 and MHC-2 was predicted using the IEDB analysis resource (<http://tools.iedb.org/population/>) [17].

Construction of Multi-epitope Vaccine

For the final vaccination, the most immunogenic, antigenic, nontoxic, and nonallergenic epitopes were chosen. As the peptides do not trigger the immune response on their own, they require an adjuvant to be attached. The adjuvant (50S ribosomal46 protein L7/L12) was chosen and added to the amino terminus. It was then linked to B cell epitopes using the EAAAK peptide, this allow efficient attachment and presentation of the adjuvant along with the B-cell epitopes [18]. The GPGPG linker is used to connect the B-cell epitope to the MHC-1 epitope in order to provide flexibility and structural integrity between these two regions of the vaccine construct, which helps maintain the structural independence of the B-cell and MHC-1 epitopes while allowing for optimal antigen presentation. Similarly, the AAY linker is employed to connect the MHC-1 epitope to the MHC-2 epitope. The purpose of this linker is to provide a suitable separation between the two epitopes, ensuring their distinct folding and interaction with their respective immune receptors. By incorporating appropriate linkers, we can optimize the spatial arrangement of different epitopes within the vaccine construct, enabling efficient recognition by B-cells, MHC-1, and MHC-2 molecules, and promoting an effective immune response [19–21].

Physiochemical Property and Solubility Prediction of Vaccine Construct

Physiochemical properties of the vaccine were predicted from ExPASy protparam server (<https://web.expasy.org/protparam/>). This server gives basic physiochemical properties like molecular weight, theoretical pI, estimated half-life, instability index, aliphatic index, and grand average of hydropathicity (GRAVY) [22]. The solubility of the vaccine was predicted by the SOLUPROT server, SoluProt is a server for the prediction of soluble protein expression in *Escherichia coli*, It has an accuracy of 58.5% or higher compared to other tools (<https://loschmidt.chemi.muni.cz/soluprot/>) [23].

Secondary Structure Prediction

The secondary structure of the vaccine construct was predicted by the PSIPRED server (<http://bioinf.cs.ucl.ac.uk/psipred/>), it is a protein structure prediction server that allows the user to input the FASTA sequence and the results are obtained as [24]. The RaptorX Property server was used to find solvent accessibility and disorder regions of the vaccine construct (<http://raptorx.uchicago.edu/>) [25].

Tertiary Structure Prediction

The tertiary structure of the vaccine was predicted by the Raptor-X server. This server gives an automated template-based tertiary structure model of proteins. The obtained model was refined with the Galaxy refine server (<https://galaxy.seoklab.org/cgi-bin/submit.cgi?type=REFINE>). Refinement is necessary as it improves the quality of the protein model, which is useful for further analysis [26].

Structure Validation

A good quality homology model is required to get optimum results hence structure validation of the homology model of the vaccine was done, The ProSA-webserver was used to find the Z-score(<https://prosa.services.came.sbg.ac.at/prosa.php>). The Z-score denotes the overall protein model quality [27]. The Ramachandran plot analysis was obtained by the Procheck server in the structure validation server (<https://saves.mbi.ucla.edu/>). The Ramachandran plot describes the quality of the three-dimensional structure of proteins and gives the amino acid residues in the most favored region, allowed region, and disallowed region [28].

Molecular Docking of the Constructed Vaccine Against TLR-8

Human parainfluenza viruses are ssRNA viruses, hence they are mainly recognized by TLR7 and TLR8 [29], hence the vaccine was docked against the TLR-8 receptor by using the Cluspro2.0 server (<https://cluspro.org/help.php>) [30]. It is a widely used server for protein-protein docking. In the receptor option, the PDB ID of TLR-8 (6ZJZ) was entered as an input, and chain A was selected. In the ligand option, the PDB file of our vaccine model was entered as an input, and other parameters were set to default, and it was docked. The interactions between the docked complex of the vaccine and TLR-8 were found by using the standalone version of PDBsum generate. The PDB file of the vaccine-TLR-8 docked complex was uploaded and an email was provided for receiving results.

Molecular Dynamic Simulation of Vaccine-TLR-8 Docked Complex

Molecular dynamic simulation is a computational method to predict how atoms in a molecular system moves over a period of time. MD simulations were carried out with the iMods server (<https://imods.iqfr.csic.es/>). It was used to obtain Deformability, B-factor, the eigenvalue of interacting residues, variance and co-variance among individual residues, and elastic network between the corresponding pairs of atoms. From these parameters, the stability of the complex was predicted [31].

In-silico Cloning for Vaccine Expression

For the expression of the vaccine in a vector, the sequence of vaccine was reverse translated with the EMBOSS Backtranseq server (https://www.ebi.ac.uk/Tools/st/emboss_backtranseq/) [32]. The obtained reverse translated sequence was subjected to codon optimization through the Java Codon Adaption tool (JCat) server (<http://www.jcat.de/>) [33]. It was done to express the vaccine in *Escherichia coli* (*E. coli* strain K12). This optimized codon was further used for cloning. The *E. coli* pET 29 (+) was selected as the expression vector. Then, by using the SnapGene tool (<https://www.snapgene.com/>) [34], the StyI and ApaLI restriction sites were inserted at the ends of the optimized vaccine codon sequence. Finally, the adapted sequence having the restriction site was inserted into the pET-28a (+) vector [35].

RESULTS AND DISCUSSION

Antigenicity, Allergenicity and Toxicity Prediction of Protein Sequence

The VaxiJen 2.0 server was used to predict the antigenicity of Fusion glycoprotein F0. It predicted an antigenicity score of 0.499, which is above the threshold value of 0.4. Allergenicity which was

predicted from the AllerTop v.2.0 server, it was found that the protein sequence was non allergenic. The ToxinPred server was used for toxicity profiling, which predicted the protein sequence was non-toxic. As all of these three parameters above showed good results, the fusion glycoprotein F0 was used for further study.

B Cell Epitopes Prediction

B-cell epitopes are the antigenic portions of the bacteria that bind to the antibody. We obtained nineteen B cell epitopes from the IEBD database and these were subjected to antigenicity and allergenicity profiling from Vaxigen 2.0 and Allertop servers, respectively. It was found that three of the B-cell epitopes listed in Table 1 were non-allergenic and had a good antigenicity score. The graphical representation of B-cell epitopes is shown in Figure 2.

Table 1. B-cell epitopes.

S.N.	Start	End	Peptide	Length	Antigenicity	Allergenicity
1	526	552	Vminsthnsppvntylesrmrnpnygn	27	0.5813	Non allergenic
2	240	264	Aniteilstikkdkdsdiydyteq	25	0.5202	Non allergenic
3	218	229	Ssnlgtigeksl	12	1.4428	Non allergenic

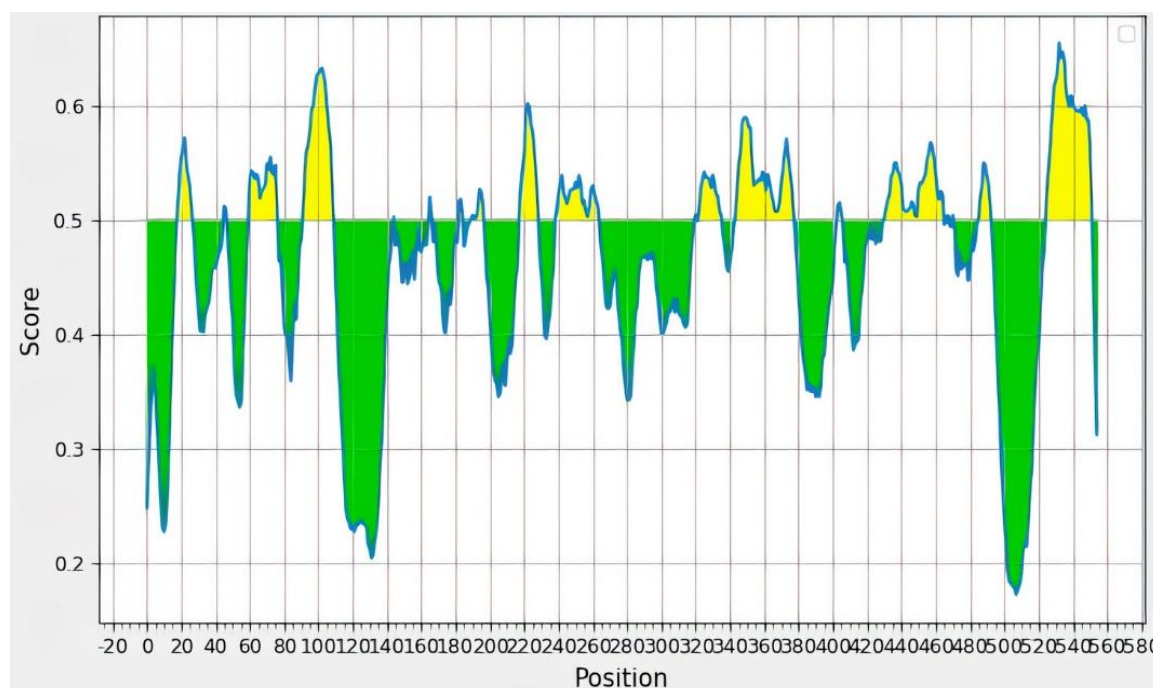


Figure 2. Graphical representation of B-cell epitopes.

Prediction of Peptide Binding to MHC Class I Molecules

To identify MHC HLA alleles in humans, we chose *Homo sapiens* as the MHC source species and used the ANN 4.0 method. This utility generates an IC50 nM value of epitopes. A lower IC50 value indicates that epitopes have a stronger affinity for the MHC Class-I molecule. A total of 942 epitopes were selected based on IC50 values less than 200 to certify a higher estimated affinity to interact with many MHC class 1 alleles. Of the 942 epitopes, 50 were chosen based on the maximal interaction of MHC

Class 1 alleles with the epitopes, epitopes were subjected for the prediction of antigenicity, allergenicity, and toxicity. Toxic and allergic epitopes with less than 0.4 antigenicity values were excluded. A total of 16 MHC class 1 epitopes were chosen for further investigation as shown in Table 2.

Table 2. Peptides binding to MHC-1

S.N.	Allele	ic50	Start	End	Length	Epitope	Antigenicity
1	HLA-A*02:03	7.19	236	245	10	SLYSANITEI	0.9188
	HLA-A*02:01	59.14					
2	HLA-A*31:01	7.26	515	523	9	LYYLYRVRR	0.5868
	HLA-A*33:01	13.37					
3	HLA-A*68:01	7.43	268	276	9	TVIDVDLEK	0.6113
	HLA-A*11:01	17.77					
4	HLA-A*02:03	8.04	277	285	9	YMTVLLVKI	0.5469
	HLA-A*02:01	10.36					
	HLA-A*02:06	13.93					
5	HLA-B*40:01	11.59	129	137	9	AQITAGIAL	0.8735
	HLA-A*02:06	15.93					
	HLA-B*15:01	29.1					
6	HLA-B*15:01	13.51	201	210	10	KLGIKLTQHY	1.4341
7	HLA-A*02:03	14.41	294	302	9	VLIYRASSI	0.5436

Prediction of Peptide Binding to MHC Class II Molecules

Using the NN-align 2.3 method, a total of 638 conserved epitopes that bind to MHC class II molecules were predicted with an IC50 of less than 200. Of those, 50 epitopes were picked and screened for antigenicity, allergenicity, and toxicity. Finally, 6 epitopes that are non-allergic, non-toxic, and have an antigenicity value of more than 0.4 were chosen for further investigation as shown in Table 3.

Table 3. Peptides binding to MHC-2.

S.N.	Alleles	ic50	Start	End	Length	Core peptide	Antigenicity
1	HLA-DRB1*04:01	12	522	536	15	LLVMINSTH	0.7626
	HLA-DRB1*04:05	23.6	519	533	15		
2	HLA-DRB1*15:01	5.8	68	82	15	IIQYKNLLN	0.5088
	HLA-DRB1*04:05	16.4	68	82	15		
3	HLA-DRB1*01:01	12.4	118	132	15	IALGVATAA	1.0766
	HLA-DRB1*09:01	9	116	130	15		
4	HLA-DQA1*01:02	27.8	129	143	15	TAGIALAEA	0.7910
	HLA-DRB1*12:01	27.8	168	182	15	IIALKTLQD	
5	HLA-DRB1*04:05	35	169	183	15	YRASSISYN	1.4051
	HLA-DRB1*01:01	26.4	169	183	15		
6	HLA-DRB1*04:01	12.9	295	309	15	YRASSISYN	1.4051
7	HLA-DRB1*01:01	61.3	257	271	15	YDIITYTEQV	0.9681

Population Coverage Analysis

Population coverage analysis was used to determine the global coverage of MHC Class-I and MHC Class-II allele interacting epitopes. It was identified by using the IEDB population coverage analysis tool. The distribution of MHC HLA alleles varies across different geographical locations across the world. As a result, population coverage is required for the development of a potentially effective vaccine. By combining alleles of MHC-I and MHC-II, we obtained population coverage of 87.47%, having an average hit of 2.58, which denotes the average number of HLA combinations recognized by the population, and a pc90 value of 0.8, which gives the minimum number of HLA combinations recognized by 90% of the population. The pictorial representation of the vaccine construct is shown in Figure 3.

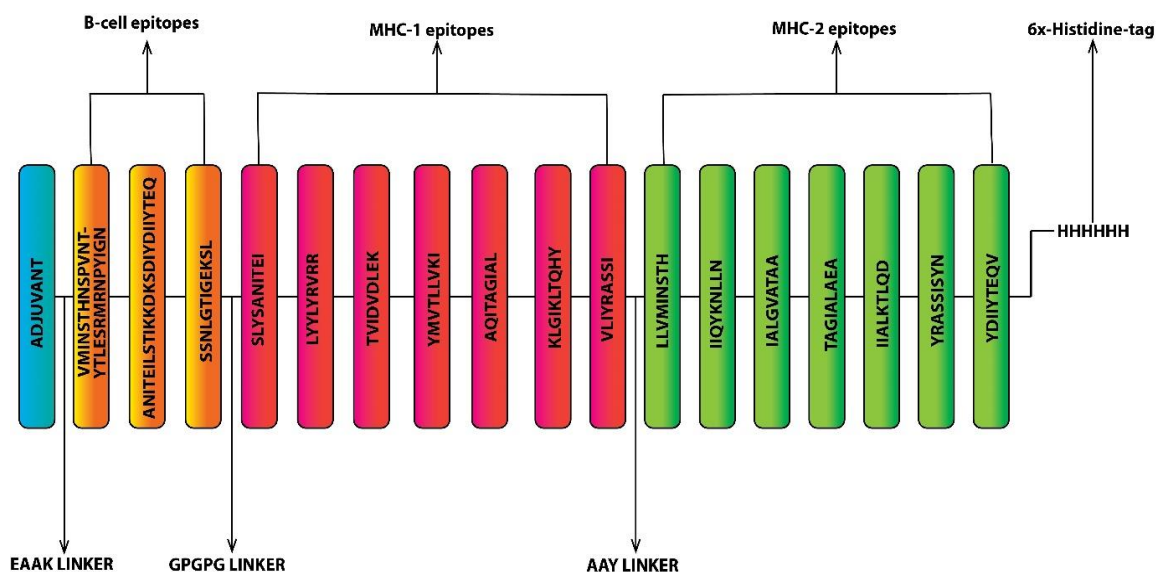


Figure 3. Pictorial representation of vaccine construct.

Construction of Multi-epitope Vaccine

The constructed multi-epitope vaccine has a sequence length of 211 amino acids, represented by the following sequence:

EAAAKVMINSTHNSPVNTYTLESRMRNPYIGNANITEILSTIKKDKSDIYDIYTEQSSNLGTIGEKSLGPGPGSLYSANITEILYLYRVRRTVIDVDLEKYMVTLVKIAQITAGIALKLGIKLTQHYVLIYRASSIAAYLLVMINSTHIIQYKNLLNIALGVATAAATAGIALAEAIALKTLQDYRASSISYNYDIYTEQVHHHHHH.

Antigenicity, Allergenicity and Toxicity Prediction of Vaccine Construct

The antigenicity, allergenicity, and toxicity of the final constructed vaccine were evaluated. The vaccine exhibited a high antigenicity score of 0.7052, surpassing the established threshold (0.4), indicating its potential to elicit an immune response. Additionally, the vaccine was found to be non-toxic and non-allergenic, further supporting its safety profile.

Physiochemical Property and Solubility Prediction of Vaccine Construct

The ExPASy ProtParam program was used to predict physiochemical characteristics. The vaccine has a molecular weight of 23472.07 Da. The theoretical PI (isoelectric point) of the vaccine obtained was 8.62, which indicates the protein is basic in nature. The instability index (II) was computed to be having a value of 38.10 denoting vaccine construct is stable. Finally, an aliphatic index value of 117.49 and the grand average of hydropathicity (GRAVY) of 0.103 were obtained. Solubility was predicted by the Soluprot server, which gave a solubility score of 0.561 indicating the vaccine is soluble in nature.

Secondary Structure Prediction of Constructed Vaccine

The secondary structure of the vaccine construct was predicted by the PSIPRED server as shown in Figure 4. The secondary structure of the vaccine obtained comprises 43.6% α -helix, 19.9% β strands, and 36.5% coil. The solvent accessibility disorder regions were predicted by using the RaptorX Property server. A total of 51% of the protein content was found to be exposed, 20% was found to be medium exposed, and 27% was found to be buried. A total of 7% of the residues were found in the disordered domain.

Tertiary Structure Prediction and Refinement of Vaccine Construct

The tertiary structure of the vaccine was predicted by using the RaptorX server. From five models obtained, we chose the first model which had the lowest RMSD (Root Mean Square Deviation) value

of the five. The 3D vaccine model obtained from RaptorX was refined using the Galaxy refine server. From five models that were obtained after refinement, we chose model 1 by considering various parameters, such as the global distance test-high accuracy score (GDT-HA) of 0.9372, which is the similarity score between protein structures. A score of more than 0.9 indicates the highest similarity, For our model, the RMSD score is used to calculate the distance between atoms, a lower RMSD number indicates higher stability. For our model, we obtained an RMSD of 0.502 and the Molprobity score represents the model's crystallographic resolution. For our model, we obtained a MolProbity score of 1.7. The value of unfavorable all-atom steric overlaps is determined by the clash score. We obtained a clash score of 6.2, which is less than the clash score of 7.7 of the initial unrefined model.

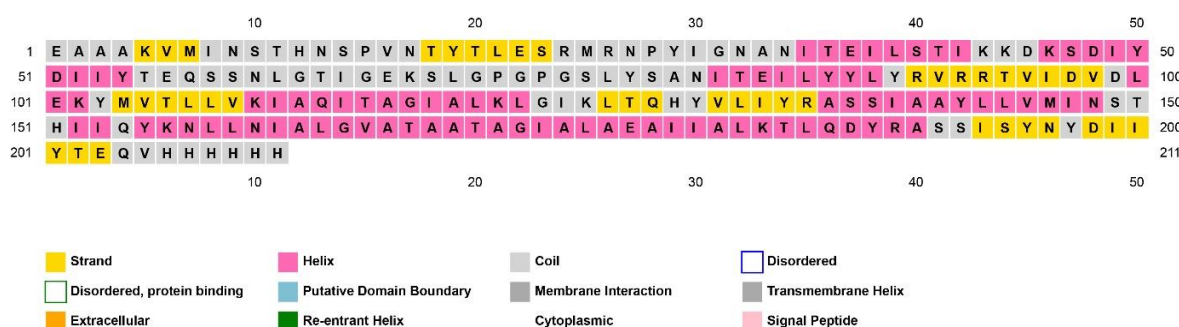


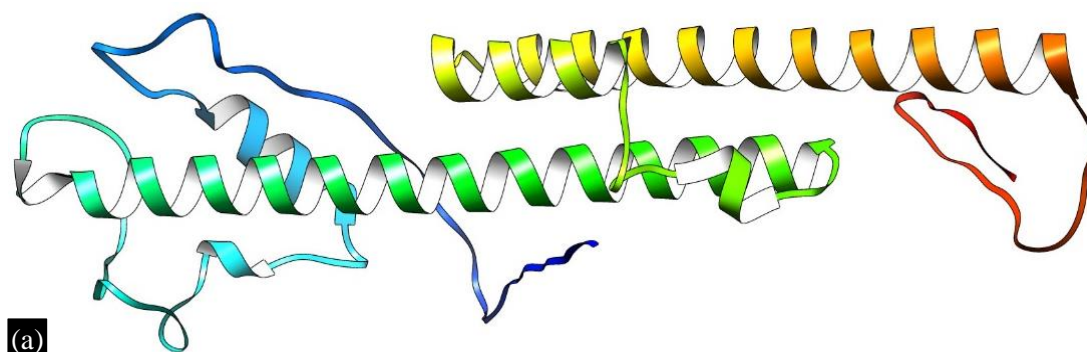
Figure 4. Secondary structure of vaccine construct.

Tertiary Structure Validation

Tertiary structure validation was done by using Prosa-web and Procheck servers as shown in Figure 5. Prosa predicts the overall model quality by giving the Z-score. For our refined vaccine model, we obtained a Z-score of 4.96 indicating good model quality. The Ramachandran plot was obtained from the PROCHECK server. According to the results, residues in the most favored regions were 89.2%, residues in allowed regions were 8.7%, and residues in disallowed regions were 2.1%. These parameters, obtained from the Ramachandran plot, indicated that the model had good quality.

Molecular Docking of Vaccine Against TLR-8

Molecular docking was done to assess the interactions between a ligand molecule and a receptor molecule to determine the stability and binding affinity of their docked complex. We chose Toll-like receptor 8 for molecular docking, as it is critical for pathogen identification and immune response. The ClusPro 2.0 server is used to perform molecular docking between the vaccine and the Chain-A of the TLR-8 receptor (PDB ID: 6ZJZ). Among all the docking models, we chose the one with the lowest energy score of -1033.4 as the best-docked complex, indicating the strong binding affinity of the vaccine to the TLR-8 receptor. The interactions between the docked complexes were found by the PDBsum server. It was found that there were 3 salt bridges, 15 hydrogen bonds, and 202 non-bonded contacts as shown in Figure 6.



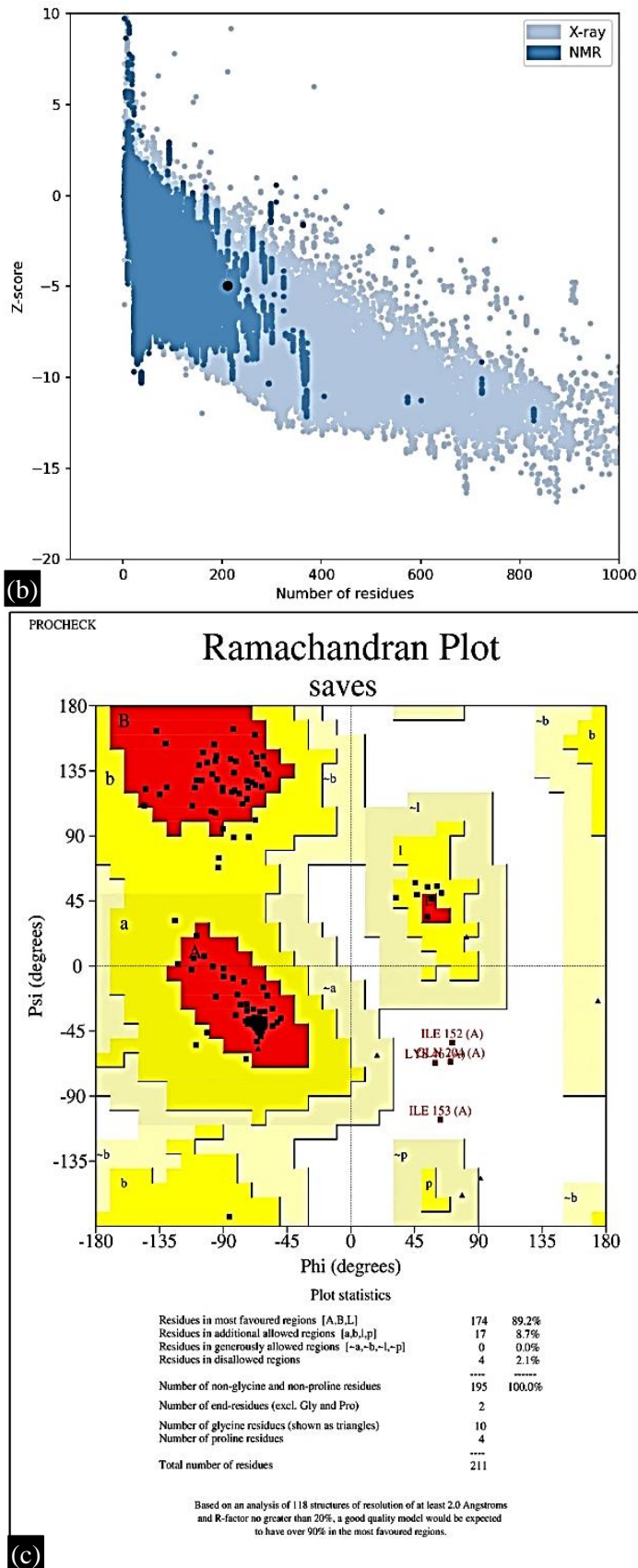


Figure 5. (a) Tertiary structure of vaccine construct, Structure validation of vaccine model by (b) Z-score graph, (c) Ramachandran plot.

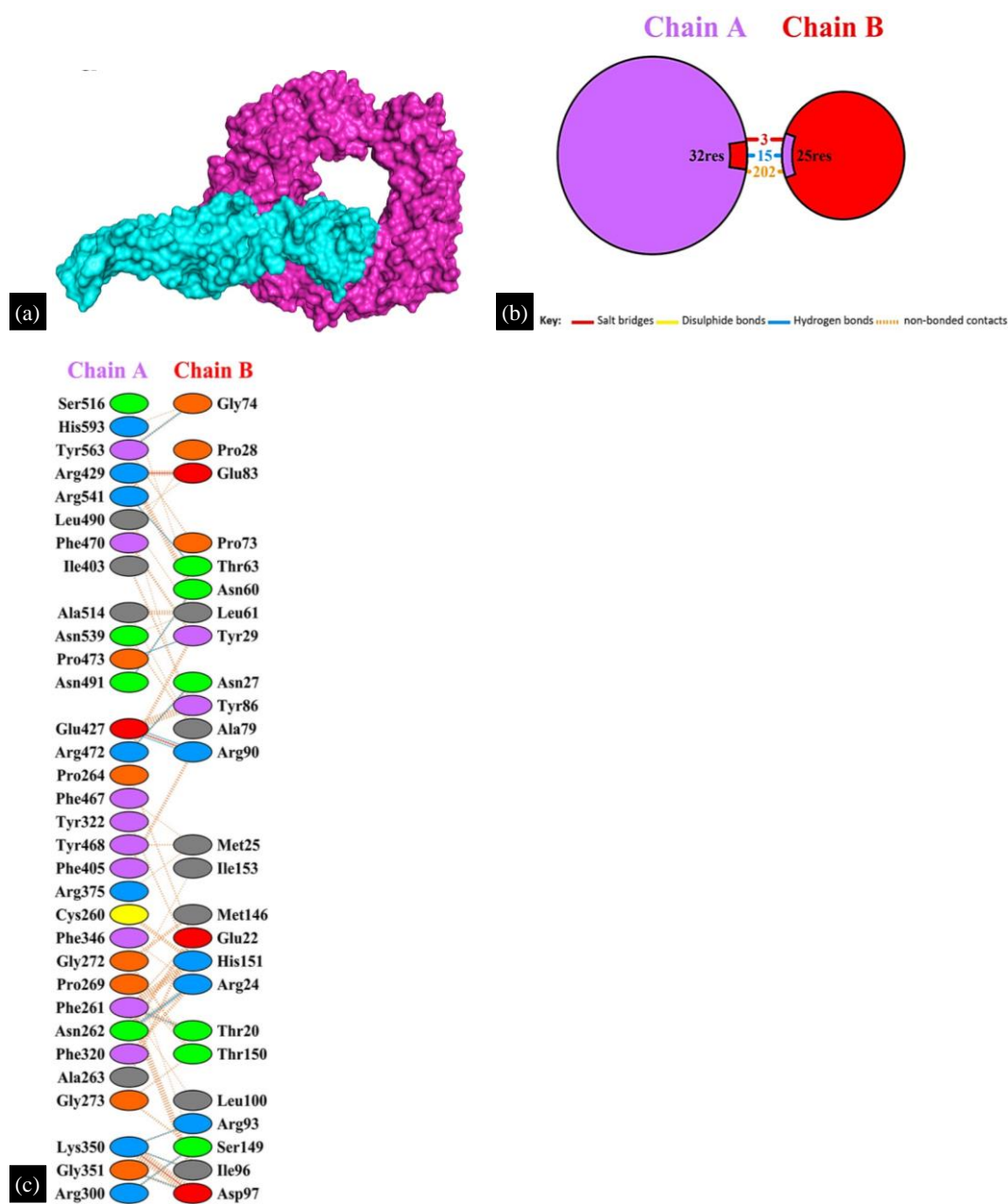


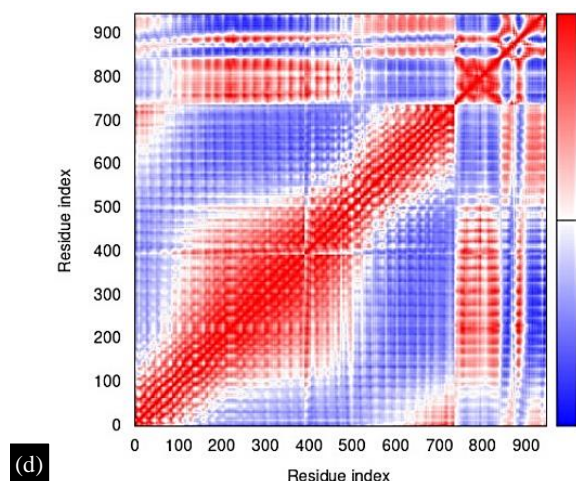
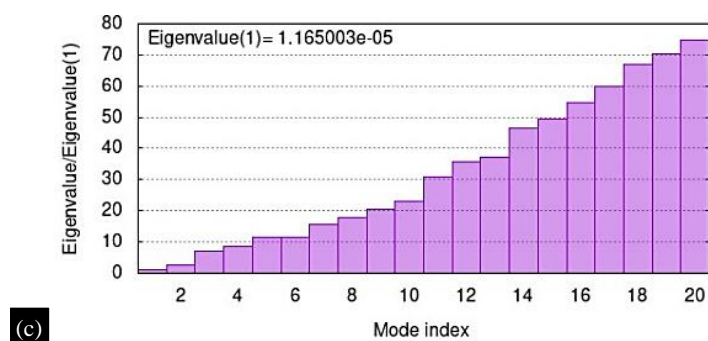
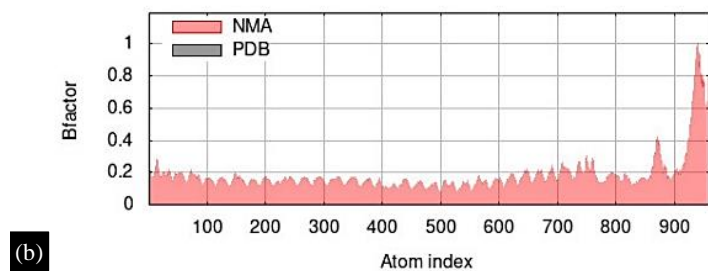
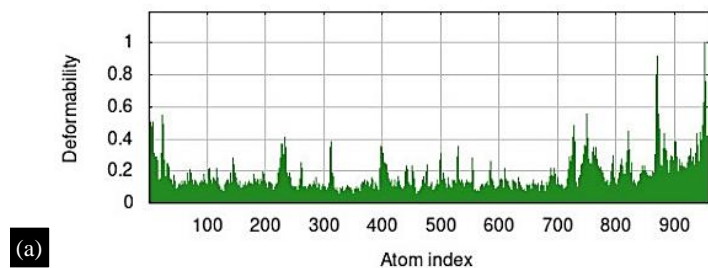
Figure 6. (a) Docked complex vaccine and TLR-8, (b) and (c) Interactions between the vaccine and TLR-8.

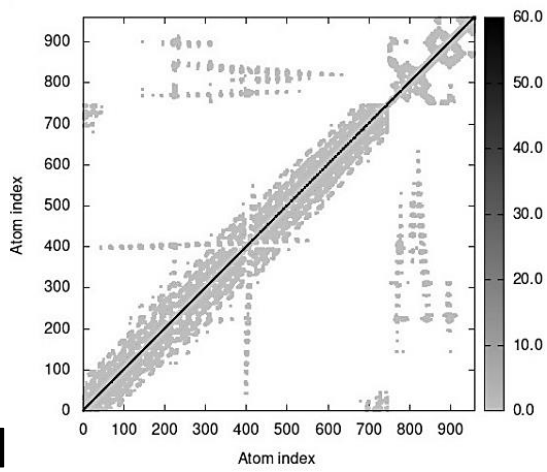
Molecular Dynamic Simulation of Vaccine-TLR-8 Docked Complex

Molecular dynamic simulations of the vaccine-TLR docked complex were analysed using the iMODS server. The results obtained are shown in Figure 7. At first, the deformability graph was obtained, which is a measure of a molecule's ability to deform at each of its residues. Then the anticipated mobilities of experimental B-factor and NMA (Normal mode analysis) were predicted. Then the eigenvalue plot was obtained, which depicts the relative stiffness of the model. The simpler the deformation, the lower the eigenvalue. We obtained an eigenvalue of $1.16500e-05$. The variance graph obtained denotes each normal mode's variance is inversely proportional to eigenvalue. Furthermore, the covariance map which shows sections of the macromolecule move in a correlated (red), uncorrelated (white), or anti-correlated (blue) pattern. Finally, an elastic network graph was obtained. The intensity of the color is depicted in relation to their stiffness; the darker the color, the stiffer the springs, and vice versa [36].

***In-silico* Clonning for Vaccine Expression**

The reverse translated vaccine sequence obtained from the EMBOSS Backtranseq server was subjected to codon optimization by using the Java codon adaptation tool (JCat) to maximize vaccine expression. The optimized codon of the vaccine had a length of 633 nucleotides, the codon adaptation index (CIA) was 0.99, and had a GC content of 61.92%. For the stable expression of a vector in *E.coli*, the optimum range of GC content should be 30–70% [37]. Finally, the adapted sequence having the restriction sites StyI and ApaLI was inserted into the pET-28a (+) vector using the Snapgene tool as shown in Figure 8.





(e)

Figure 7. (a) Deformability, (b) Experimental B-factor and NMA, (c) Eigenvalue plot, (d) Covariance map, (e) Elastic network graph.

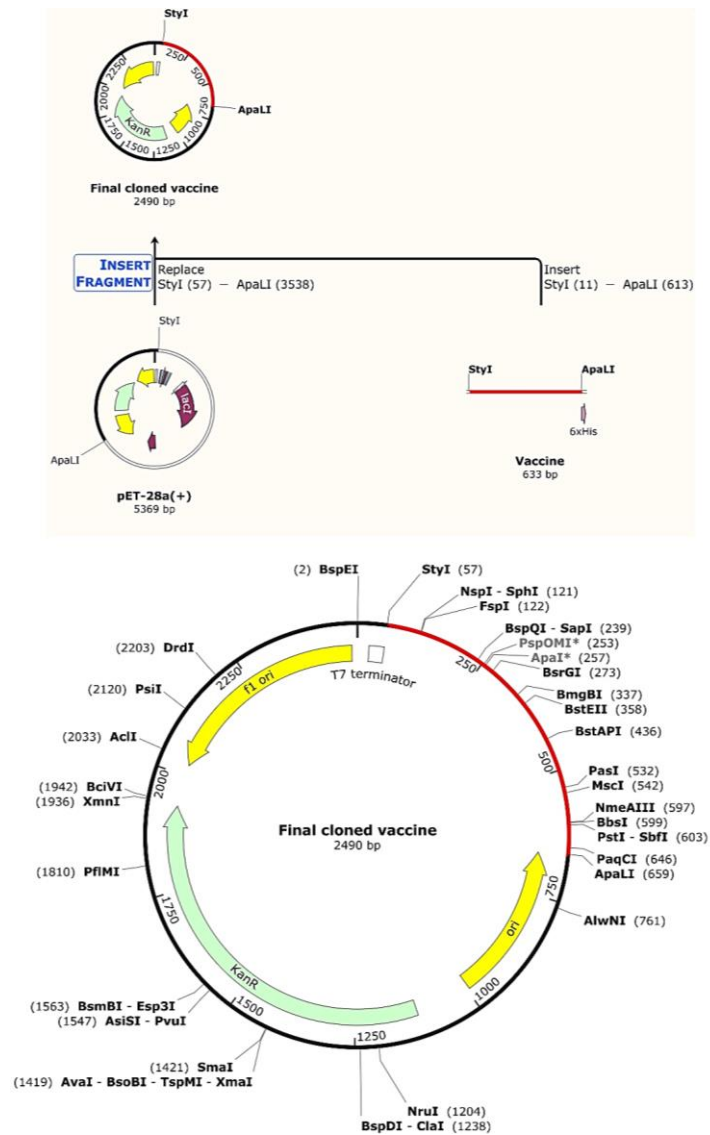


Figure 8. *In-silico* cloning of vaccine to pET-28a (+) vector.

DISCUSSION

Respiratory viruses are a leading cause of illness and mortality among children worldwide, with acute respiratory infections posing a significant threat, particularly in young children. Human parainfluenza viruses (HPIVs) are responsible for acute respiratory infections across all age groups, with higher incidence observed in small children and immunocompromised individuals [38]. HPIVs belong to the family Paramyxoviridae and comprise four species: HPIV-1, HPIV-2, HPIV-3, and HPIV-4. The virus possesses two surface proteins, hemagglutinin-neuraminidase (HN) and fusion (F), which play crucial roles in viral attachment, envelope fusion, and antibody targeting. The nucleocapsid is formed by the N protein, while the P and L proteins are associated with the nucleocapsid, and the matrix protein (M) protects the envelope's inner surface.

The pathogenesis of HPIV infections involves direct contact or airborne transmission from infected individuals, with viral attachment and replication occurring in the ciliated epithelial cells of the respiratory tract, leading to the manifestation of symptoms [39].

The clinical presentation of HPIV infections includes fever, cough, runny nose, chest pain, sore throat, shortness of breath, and respiratory difficulties. Notably, approximately 10% of all hospitalizations for acute respiratory infections in children under five years of age can be attributed to HPIV infections. HPIV-1 and HPIV-2 are the main causes of laryngotracheobronchitis, commonly known as "croup," accounting for around 75% of croup cases. Unfortunately, there are currently no effective antiviral medications or approved vaccines available for HPIV infections. To address this gap, an in-silico approach was employed to design a novel multi-epitope vaccine candidate against HPIV [40].

The Fusion (F) glycoprotein of HPIV-1, which represents a critical target for neutralizing antibodies, was selected as the antigen for vaccine development. The FASTA sequence of the F protein was retrieved from the Uniprot database and subjected to antigenicity, allergenicity, and toxicity screening, demonstrating its non-allergenic, non-toxic, and highly antigenic nature. B-cell, MHC-1, and MHC-2 epitopes of the antigen were predicted using The Immune Epitope Database (IEDB), and those epitopes that fulfilled non-allergenic, non-toxic, and high antigenicity criteria were chosen for vaccine construction. The resulting vaccine exhibited a global population coverage of 87.47% [41].

Since peptides alone do not elicit a robust immunological response, an adjuvant, 50S ribosomal protein L7/L12, was selected and added at the amino terminus. B-cell epitopes were connected using an EAAAK linker, MHC-1 epitopes with GPGPG linkers, and MHC-2 epitopes with AAY linkers. The constructed vaccine exhibited favourable physicochemical properties, including a total of 211 amino acids, a molecular weight of 23472.07 Da, an instability index (II) of 38.10, an aliphatic index of 117.49, and a grand average of hydropathicity (GRAVY) value of 0.103. Solubility analysis using the Soluprot server predicted a good solubility score of 0.561. Furthermore, secondary structure prediction using the PSIPRED server indicated 43.6% alpha-helix, 19.9% beta-strands, and 36.5% coils. The tertiary structure of the vaccine was predicted using the RaptorX server and refined through the Galaxyrefine server, with subsequent validation using the Prosa-web and Procheck servers confirming the model's quality.

Considering that human parainfluenza viruses are primarily recognized by Toll-like receptors (TLR) 7 and 8, the refined vaccine model was docked against the TLR-8 receptor using the Cluspro2.0 server. The docking analysis, supported by PDBsum, revealed three salt bridges, 15 hydrogen bonds, and 202 non-bonded contacts, indicating a high binding affinity between the vaccine and the TLR-8 receptor. To assess the stability of the vaccine-TLR-8 docked complex, molecular dynamics simulations were performed using the iMods server, which demonstrated stable and flexible interactions.

To enhance vaccine expression, the reverse-translated vaccine sequence obtained from the EMBOSS Backtranseq server underwent codon optimization using the Java Codon Adaptation Tool (JCat). The optimized codon exhibited a length of 633 nucleotides, a codon adaptation index (CIA) of 0.99, and a

GC content of 61.92%. Finally, the modified sequence, flanked by StyI and ApaLI restriction sites, was inserted into the pET-28a (+) vector using the Snapgene program [42, 43].

CONCLUSION

In conclusion, our study successfully developed a multi-epitope subunit vaccine against HPIV-1 using an in-silico approach. The selection of the Fusion glycoprotein antigen and subsequent prediction of B-cell, MHC-1, and MHC-2 epitopes allowed us to identify non-allergenic, non-toxic, and highly antigenic epitopes for vaccine construction. The physiochemical properties of the vaccine demonstrated its suitability for further development. The prediction of secondary and tertiary structures revealed a well-defined 3D model, exhibiting strong binding affinity for the human TLR-8 receptor. Molecular dynamic simulations confirmed the stability of the vaccine-TLR-8 docked complex, providing additional support for its potential effectiveness. However, it is important to note that our study solely employed in-silico techniques, and further in vitro and in vivo investigations are essential to evaluate the vaccine's efficacy, immunogenicity, and host safety. These experimental studies will provide critical insights before advancing the vaccine candidate for potential administration to humans. In summary, our in-silico multi-epitope vaccine design offers a promising foundation for future research and development efforts aimed at combating HPIV-1 infections. Continued exploration and validation of this vaccine candidate hold great potential for the prevention and control of HPIV-1, ultimately benefiting public health.

Abbreviations

F: Fusion glycoprotein (F); GRAVY: Grand average of hydropathicity; HLA: Human leukocyte antigens; HN: Hemagglutinin-neuraminidase glycoprotein; HPIV: Human parainfluenza viruses; IC50: Half-maximal inhibitory concentration; IEDB: Immune Epitope Database; JCat: Java Codon Adaptation Tool; L: RNA polymerase; M: Matrix protein; MHC: Major histocompatibility complex; NMA: Normal mode analysis; NP: Nucleocapsid protein; P: Phosphoprotein; PDB: Protein data bank; PI: Isoelectric point; RNA: Ribonucleic acid; TLR: Toll-like receptor

REFERENCES

1. Branche AR, Falsey AR (2016) Parainfluenza virus infection. *Semin Respir Crit Care Med* 37:538–54. <https://doi.org/10.1055/s-0036-1584798>
2. Elboukari H, Ashraf M (2023) Parainfluenza Virus. StatPearls Publishing
3. Slobod KS, Shenep JL, Luján-Zilbermann J, Allison K, Brown B, Scroggs RA, Portner A, Coleclough C, Hurwitz JL (2004) Safety and immunogenicity of intranasal murine parainfluenza virus type 1 (Sendai virus) in healthy human adults. *Vaccine* 22:3182-3186. <https://doi.org/10.1016/j.vaccine.2004.01.053>
4. Smith CB, Purcell RH, Bellanti JA, Chanock RM, Laine P (1966) Protective effect of antibody to parainfluenza type 1 virus. *N Engl J Med* 275:1145-1152. <https://doi.org/10.1056/nejm.196611242752101>
5. Pawełczyk M, Kowalski ML (2017) The Role of Human Parainfluenza Virus Infections in the Immunopathology of the Respiratory Tract. *Curr Allergy Asthma Rep* 17:1-10. <https://doi.org/10.1007/s11882-017-0685-2>
6. Schomacker H, Schaap-Nutt A, Collins PL, Schmidt AC (2012). Pathogenesis of acute respiratory illness caused by human parainfluenza viruses. *Curr Opin Virol* 2:294-299. <https://doi.org/10.1016/j.coviro.2012.02.001>
7. Moscona A (2005) Entry of parainfluenza virus into cells as a target for interrupting childhood respiratory disease. *J. Clin. Invest* 115:1688–1698. <https://doi.org/10.1172/jci25669>
8. Henrickson KJ (2003) Parainfluenza viruses. *Clin Microbiol Rev* 16:242-264. <https://doi.org/10.1128/cmr.16.2.242-264.2003>
9. Russell CJ, Simões EAF, Hurwitz JL (2018) Vaccines for the Paramyxoviruses and Pneumoviruses: Successes, Candidates, and Hurdles. *Viral Immunol* 31:133–141. <https://doi.org/10.1089/vim.2017.0137>

10. van Wyke Coelingh K, Tierney EL (1989) Antigenic and functional organization of human parainfluenza virus type 3 fusion glycoprotein. *J Virol* 63:375-382. <https://doi.org/10.1128/jvi.63.1.375-382.1989>
11. Wang Y, Wang Q, Huang H, Huang W, Chen Y, McGarvey PB, Wu CH, Arighi CN (2021). A crowdsourcing open platform for literature curation in UniProt. *PLoS Biol* 19:e3001464. <https://doi.org/10.1371/journal.pbio.3001464>
12. Doytchinova IA, Flower DR (2007). VaxiJen: a server for prediction of protective antigens, tumour antigens and subunit vaccines. *BMC Bioinformatics* 8:1-7. <https://doi.org/10.1186/1471-2105-8-4>
13. Dimitrov I, Bangov I, Flower DR, Doytchinova I (2014). AllerTOP v. 2—a server for in silico prediction of allergens. *J Mol Model* 20:1-6. <https://doi.org/10.1007/s00894-014-2278-5>
14. Xiao X, Wu Z-C, Chou K-C (2011). A multi-label classifier for predicting the subcellular localization of gram-negative bacterial proteins with both single and multiple sites. *PLoS One* 6:e20592. <https://doi.org/10.1371/journal.pone.0020592>
15. Jespersen MC, Peters B, Nielsen M, Marcatili P (2017) BepiPred-2.0: improving sequence-based B-cell epitope prediction using conformational epitopes. *Nucleic Acids Res* 45:W24-W29. <https://doi.org/10.1093/nar/gkx346>
16. Vita R, Mahajan S, Overton JA, Dhanda SK, Martini S, Cantrell JR, Wheeler DK, Sette A, Peters B (2019) The immune epitope database (IEDB): 2018 update. *Nucleic Acids Res* 47:D339-D343. <https://doi.org/10.1093/nar/gky1006>
17. Yan F, Polk DB (2020) Probiotics and probiotic-derived functional factors—mechanistic insights into applications for intestinal homeostasis. *Front Immunol* 11:1428. <https://doi.org/10.3389/fimmu.2020.01428>
18. Naveed M, Tehreem S, Arshad S, Bukhari SA, Shabbir MA, Essa R, Ali N, Zaib S, Khan A, Al-Harrasi A, Khan I (2021) Design of a novel multiple epitope-based vaccine: An immunoinformatics approach to combat SARS-CoV-2 strains. *J Infect Public Health* 14:938-946. <https://doi.org/10.1016/j.jiph.2021.04.010>
19. Dong R, Chu Z, Yu F, Zha Y (2020) Contriving Multi-Epitope Subunit of Vaccine for COVID-19: Immunoinformatics Approaches. *Front Immunol* 11:1784. <https://doi.org/10.3389/fimmu.2020.01784>
20. Hasan M, Mia M (2022) Exploratory Algorithm of a Multi-epitope-based Subunit Vaccine Candidate Against *Cryptosporidium hominis*: Reverse Vaccinology-Based Immunoinformatic Approach. *Int J Pept Res Ther* 28(5):134. <https://doi.org/10.1007/s10989-022-10438-6>
21. Maleki A, Russo G, Parasiliti Palumbo GA, Pappalardo F (2022) In silico design of recombinant multi-epitope vaccine against influenza A virus. *BMC Bioinform* 22(14):1-18. <https://doi.org/10.1186/s12859-022-04581-6>
22. Gasteiger E, Hoogland C, Gattiker A, Wilkins MR, Appel RD, Bairoch A (2005) Protein identification and analysis tools on the ExPASy server. *Springer Protocols Handbooks*. Humana press 571-607. <https://doi.org/10.1385/1-59259-890-0:571>
23. Hon J, Marusiak M, Martinek T, Zendulka J, Bednar D, Damborsky J (2021) SoluProt: prediction of soluble protein expression in *Escherichia coli*. *Bioinformatics* 37:23-28. <https://doi.org/10.1093/bioinformatics/btaa1102>
24. Jones DT (1999) Protein secondary structure prediction based on position-specific scoring matrices. *J Mol Biol* 292:195-202. <https://doi.org/10.1006/jmbi.1999.3091>
25. Wang S, Li W, Liu S, Xu J (2016) RaptorX-Property: a web server for protein structure property prediction. *Nucleic Acids Res* 44:W430-W435. <https://doi.org/10.1093/nar/gkw306>
26. Ko J, Park H, Heo L, Seok C (2012) GalaxyWEB server for protein structure prediction and refinement. *Nucleic Acids Res* 40:W294-W297. <https://doi.org/10.1093/nar/gks493>
27. Wiederstein M, Sippl MJ (2007). ProSA-web: interactive web service for the recognition of errors in three-dimensional structures of proteins. *Nucleic Acids Res* 35:W407-W410. <https://doi.org/10.1093/nar/gkm290>
28. Laskowski RA, MacArthur MW, Moss DS, Thornton JM (1993) PROCHECK: a program to check the stereochemical quality of protein structures. *J. Appl. Cryst* 26:283-291. <https://doi.org/10.1107/s0021889892009944>

29. Xagorari A, Chlichlia K (2008) Toll-like receptors and viruses: induction of innate antiviral immune responses. *Open Microbiol J* 2:49. <https://doi.org/10.2174/1874285800802010049>
30. Desta IT, Porter KA, Xia B, Kozakov D, Vajda S (2020) Performance and its limits in rigid body protein-protein docking. *Structure* 28:1071-1081.e1073. <https://doi.org/10.1016/j.str.2020.06.006>
31. López-Blanco JR, Aliaga JI, Quintana-Ortí ES, Chacón (2014) iMODS: internal coordinates normal mode analysis server. *Nucleic Acids Res* 42:W271-W276. <https://doi.org/10.1093/nar/gku339>
32. Rice P, Longden I, Bleasby (2000) EMBOSS: the European molecular biology open software suite. *Trends Genet* 16:276-277. [https://doi.org/10.1016/s0168-9525\(00\)02024-2](https://doi.org/10.1016/s0168-9525(00)02024-2)
33. Grote A, Hiller K, Scheer M, Münch R, Nörtemann B, Hempel DC, Jahn D (2005) JCat: a novel tool to adapt codon usage of a target gene to its potential expression host. *Nucleic Acids Res* 33:W526-W531. <https://doi.org/10.1093/nar/gki376>
34. Samad A, Ahammad F, Nain Z, Alam R, Imon RR, Hasan M, Rahman MS (2022) Designing a multi-epitope vaccine against SARS-CoV-2: An immunoinformatics approach. *J Biomol Struct Dyn* 40:14-30. <https://doi.org/10.1080/07391102.2020.1792347>
35. Yang Z, Bogdan P, Nazarian (2021) An in silico deep learning approach to multi-epitope vaccine design: a SARS-CoV-2 case study. *Sci Rep* 11:1-21. <https://doi.org/10.21203/rs.3.rs-36528/v1>
36. Naveed M, Yaseen AR, Khalid H, Ali U, Rabaan AA, Garout M, Halwani MA, Al Mutair A, Alhumaid S, Al Alawi Z, Alhashem YN (2022) Execution and Design of an Anti HPIV-1 Vaccine with Multiple Epitopes Triggering Innate and Adaptive Immune Responses: An Immunoinformatic Approach. *Vaccines* 10:869. <https://doi.org/10.3390/vaccines10060869>
37. Khatoun N, Pandey RK, Prajapati VK (2017) Exploring Leishmania secretory proteins to design B and T cell multi-epitope subunit vaccine using immunoinformatics approach. *Sci Rep* 7:1-12. <https://doi.org/10.1038/s41598-017-08842-w>
38. Howard LM, Rankin DA, Spieker AJ, Gu W, Haddadin Z, Probst V, Rahman H, McHenry R, Pulido CG, Williams JV, Faouri S (2021) Clinical features of parainfluenza infections among young children hospitalized for acute respiratory illness in Amman, Jordan. *BMC Infect Dis* 2:1-9. <https://doi.org/10.1186/s12879-021-06001-1>
39. Marcink TC, Porotto M, Moscona A (2021) Parainfluenza virus entry at the onset of infection. *Adv Virus Res* 111:1–29. <https://doi.org/10.1016/bs.aivir.2021.07.001>
40. Linster M, Do LA, Minh NN, Chen Y, Zhe Z, Tuan TA, Tuan HM, Su YC, van Doorn HR, Moorthy M, Smith GJ (2018) Clinical and molecular epidemiology of human parainfluenza viruses 1–4 in children from Viet Nam. *Sci Rep* 8:1-8. <https://doi.org/10.1038/s41598-018-24767-4>
41. Nelluri KDD, Ammulu MA, Durga ML, Sravani M, Kumar VP, Poda S (2022) In silico multi-epitope Bunyavirus vaccine to target virus nucleocapsid N protein. *J Genet Eng Biotechnol* 20(1):89. <https://doi.org/10.1186/s43141-022-00355-y>
42. Akhtar N, Singh A, Upadhyay AK, Mannan MA (2022) Design of a multi-epitope vaccine against the pathogenic fungi *Candida tropicalis* using an in silico approach. *J Genet Eng Biotechnol* 20:140. <https://doi.org/10.1186/s43141-022-00415-3>
43. Shahab M, Hayat C, Sikandar R, Zheng G, Akter S (2022) In silico designing of a multi-epitope vaccine against *Burkholderia pseudomallei*: reverse vaccinology and immunoinformatics. *J Genet Eng Biotechnol* 20:100. <https://doi.org/10.1186/s43141-022-00379-4>